



Contents lists available at SciVerse ScienceDirect

Neurobiology of Aging

journal homepage: www.elsevier.com/locate/neuagingDeregulation of calcium homeostasis mediates secreted α -synuclein-induced neurotoxicityKaterina Melachroinou^a, Maria Xilouri^a, Evangelia Emmanouilidou^a, Roser Masgrau^b, Panagiota Papazafiri^c, Leonidas Stefanis^{a,d}, Kostas Vekrellis^{a,*}^a Division of Basic Neurosciences, Biomedical Research Foundation of the Academy of Athens, Athens, Greece^b Departament de Bioquímica i Biologia Molecular, and Institut de Neurociències, Universitat Autònoma de Barcelona, Barcelona, Catalonia, Spain^c Division of Animal and Human Physiology, Department of Biology, University of Athens, Athens, Greece^d Second Department of Neurology, University of Athens Medical School, Athens, Greece

ARTICLE INFO

Article history:

Received 22 January 2013

Received in revised form 4 June 2013

Accepted 14 June 2013

Keywords:

Parkinson's disease

Alpha-synuclein

Secretion

Exosomes

Calpains

Membrane fluidity

Mitochondria

Neurodegeneration

ABSTRACT

α -Synuclein (AS) plays a crucial role in Parkinson's disease pathogenesis. AS is normally secreted from neuronal cells and can thus exert paracrine effects. We have previously demonstrated that naturally secreted AS species, derived from SH-SY5Y cells inducibly overexpressing human wild type AS, can be toxic to recipient neuronal cells. In the current study, we show that application of secreted AS alters membrane fluidity and increases calcium (Ca^{2+}) entry. This influx is reduced on pharmacological inhibition of voltage-operated Ca^{2+} channels. Although no change in free cytosolic Ca^{2+} levels is observed, a significantly increased mitochondrial Ca^{2+} sequestration is found in recipient cells. Application of voltage-operated Ca^{2+} channel blockers or Ca^{2+} chelators abolishes AS-mediated toxicity. AS-treated cells exhibit increased calpain activation, and calpain inhibition greatly alleviates the observed toxicity. Collectively, our data suggest that secreted AS exerts toxicity through engagement, at least in part, of the Ca^{2+} homeostatic machinery. Therefore, manipulating Ca^{2+} signaling pathways might represent a potential therapeutic strategy for Parkinson's disease.

© 2013 Elsevier Inc. All rights reserved.

1. Introduction

The pathological hallmark of Parkinson's disease (PD) is the loss of the dopaminergic neurons primarily in the substantia nigra pars compacta and the presence of proteinaceous inclusions, termed Lewy bodies and Lewy neurites, in the somata or axons, respectively, of the remaining neurons (Dauer and Przedborski, 2003; Spillantini et al., 1997). The primary structural component of these intraneuronal aggregates is α -synuclein (AS), a small acidic protein that is mainly found in presynaptic terminals. AS is genetically linked to familial and sporadic disease (Gasser, 2009; Nalls et al., 2011). Importantly, AS is detected in human biological fluids and in the culture medium of neuronal cells, suggesting a possible paracrine mode of action in the extracellular milieu (Vekrellis et al., 2011). AS has been found to be secreted, via a nonclassical, calcium-dependent mechanism that partly relies on exosomes (Emmanouilidou et al., 2010), small extracellular vesicles

which derive from endosomes after fusing with the plasma membrane (Chivet et al., 2012). Extracellular AS can be toxic to recipient cells, and has assumed an augmented importance, for the reason that it might be involved in disease propagation, otherwise known as 'spreading' in the context of PD (Kordower et al., 2008; Li et al., 2008).

It has been shown that aberrant forms of recombinant AS (oligomers, aggregates) can create pores that compromise plasma membrane integrity, much like other aggregating-prone proteins such as amyloid beta peptide and prion (Danzer et al., 2007; Tsigelny et al., 2012). Alternatively, such proteins can interact with calcium (Ca^{2+}) channels, thereby altering their function and compromising Ca^{2+} equilibrium between intracellular and extracellular spaces (Demuro et al., 2010). Ca^{2+} ions play a pivotal role in neuronal plasticity and survival (Berridge et al., 2003; Greer and Greenberg, 2008); thus, an extremely complex homeostatic network operates to regulate intracellular Ca^{2+} levels. Ca^{2+} influx has long been considered as a key source of Ca^{2+} signals, and together with Ca^{2+} release from internal stores, such as the endoplasmic reticulum (ER), plays a major role in Ca^{2+} homeostasis (Patel and Docampo, 2010). Acidic organelles have also been shown to be intracellular Ca^{2+} stores (Churchill et al., 2002; Yamasaki et al., 2004) and

* Corresponding author at: Division of Basic Neurosciences, Biomedical Research Foundation of the Academy of Athens (BRFAA), 4, Soranou Efessiou Street, Athens 11527, Greece. Tel.: +30 210 6597523; fax: +30 210 6597545.

E-mail address: vekrellis@bioacademy.gr (K. Vekrellis).

emerging evidence highlights their important role in Ca^{2+} signaling and cell physiology (Patel and Docampo, 2010). Additionally, mitochondria play a very important role on Ca^{2+} signaling, being physically and functionally linked to the ER, thus shaping intracellular Ca^{2+} responses (de Brito and Scorrano, 2008; Lamarca and Scorrano, 2009).

Deregulation of Ca^{2+} homeostasis has been recently proposed as a major age-related condition driving neurodegeneration in sporadic PD (Zundorf and Reiser, 2011). This view is supported by the finding that dopaminergic neurons expressing higher levels of Ca^{2+} -binding proteins, such as calbindin D28K, calretinin, and parvalbumin, seem to be resistant to degeneration in PD (Surmeier et al., 2010). Moreover, recombinant AS has been shown to trigger Ca^{2+} influx and induce caspase activation in a variety of neuronal systems (Danzon et al., 2007; Furukawa et al., 2006; Martin et al., 2012). However, the effects of cell-derived naturally secreted AS on Ca^{2+} homeostasis in a neuronal cell context have not been assessed.

To address this issue, we have used the human SH-SY5Y neuroblastoma cell line, in which the expression of human wild type (WT) AS can be induced, as a source of naturally secreted AS (Vekrellis et al., 2009). We have previously shown that these cells readily secrete a wide range of AS species, which are toxic to recipient neuronal cells (Emmanouilidou et al., 2010). Here, we show that application of medium enriched in secreted AS on neuronally differentiated SH-SY5Y cells and primary rat cortical neurons, is accompanied by perturbation of Ca^{2+} homeostasis and neuronal death. These effects are ameliorated by blockage of voltage-operated Ca^{2+} channels (VOCs), Ca^{2+} chelation, or calpain inhibition. The increase in Ca^{2+} influx is mostly attributed to free extracellular, rather than exosome-associated AS. We further show that extracellular AS alters membrane fluidity properties of the recipient cells, and evokes Ca^{2+} sequestration into the mitochondria. Collectively, our data suggest that secreted AS is toxic to recipient neuronal cells, at least in part, through the disruption of the Ca^{2+} homeostatic machinery.

2. Methods

2.1. Reagents

Reagents were obtained from Sigma-Aldrich (St Louis, MO, USA) unless otherwise specified. G agarose beads, Fluorogenic Substrate IV, and Fura 2-AM calcium indicator were purchased from Calbiochem (San Diego, CA, USA). Carbonyl cyanide p-trifluoromethoxyphenylhydrazone (FCCP), ω -conotoxin GVIA (cntx) and SKF 96365 hydrochloride (SKF) were purchased from Tocris Bioscience. 1-Pyrenedodecanoic acid was obtained from Molecular Probes/Invitrogen (Eugene, OR, USA).

2.2. Cell culture

Stable SH-SY5Y cell lines inducibly expressing WT AS were generated as previously described (Vekrellis et al., 2009). Cells were cultured in RPMI 1640 medium containing 10% fetal bovine serum (FBS), penicillin (100 U/mL), streptomycin (100 $\mu\text{g}/\text{mL}$), and 2 mM L-glutamine. AS expression was switched off by the addition of doxycycline (dox) (1.0 $\mu\text{g}/\text{mL}$). Neuronal differentiation was performed with the addition of 10 μM all-trans retinoic acid for 6 days. Cultures of rat (embryonic day 18) cortical neurons were prepared as previously described (Vogiatzi et al., 2008). Dissociated cells were plated onto poly-D-lysine-coated 24-well dishes at a density of 150,000–200,000 cells per cm^2 and maintained in Neurobasal medium (Gibco, Invitrogen), containing 2% B27 supplement (Gibco, Invitrogen), 0.5 mM L-glutamine, and 1% penicillin/streptomycin.

2.3. Preparation of conditioned medium

SH-SY5Y cells inducibly expressing WT AS were cultured in 140 mm dishes in RPMI medium containing 10% FBS in the presence (1.0 $\mu\text{g}/\text{mL}$) or absence of dox until 70%–80% confluency was reached. The medium was then replaced with RPMI containing 2% FBS. After 48 hours, the culture supernatant (conditioned medium [CM]) was collected and centrifuged sequentially at 400g for 5 minutes at 4 °C to remove unbroken cells and at 4000g for 10 minutes at 4 °C to remove cell debris.

2.4. Exosome purification

Before use, FBS exosomes were depleted from the culture medium as described previously (Thery et al., 2006). Before exosome isolation, the culture medium of SH-SY5Y cells was replaced with exosome-depleted medium diluted 10-fold with RPMI containing only penicillin/streptomycin and L-glutamine for 48 hours. The culture supernatant was collected and sequentially centrifuged at 400g for 10 minutes, and at 2000g for 10 minutes, 10,000g for 30 minutes, and 100,000g for 90 minutes. The obtained pellet (P100) containing mostly exosomes was washed once with ice-cold phosphate buffered saline (PBS) and centrifuged again at 100,000g for 90 minutes. The final P100 pellet was resuspended in PBS buffer or lysed in radioimmunoprecipitation assay (RIPA) buffer.

2.5. Immunodepletion of AS from CM

AS was immunodepleted from CM as described previously (Emmanouilidou et al., 2010). The anti-AS antibody (Syn-1, mouse monoclonal; BD Biosciences; 0.5 μg antibody per mL CM) was used to immunoprecipitate AS from the CM overnight. Immunodepleted CM was collected and sterilized through a 0.2 μm filter (Whatman) before application to recipient cells. Control immunodepletion was performed using an anti-c-myc antibody of the same isotype (mouse monoclonal; Santa Cruz Biotechnology).

2.6. Western blot analysis

For Western blot analysis, CM and exosome-depleted supernatants (S100) were concentrated using 3-kDa cutoff Amicon Ultra filters (Millipore). The P100 containing exosomes was reconstituted in 25 μL of RIPA buffer (50 mM Tris-HCl, pH 7.6, 150 mM NaCl, 1% NP-40, 0.5% Na deoxycholate, and 0.1% sodium dodecyl sulfate). Denaturing gel electrophoresis was performed in 12% sodium dodecyl sulfate polyacrylamide gel electrophoresis gels in Tris-glycine buffer. Immunoblot analysis was performed using the following antibodies: anti-AS (rabbit polyclonal; C-20), anti-bovine serum albumin (anti-BSA) (mouse monoclonal), anti-Alix (mouse monoclonal), and anti-Flotillin (mouse monoclonal). All antibodies were from Santa Cruz Biotechnology.

2.7. Assessment of survival

Six-day differentiated SH-SY5Y neuroblastoma cells or 7-day-old rat cortical neurons were treated with AS-containing (CM, WT–) or control (CM, WT+) CM in the presence or absence of Ca^{2+} modulators or calpain inhibitors. Concentrations of the compounds are mentioned in the figures. Recipient cells were lysed in a detergent-containing solution, which enables the quantification of viable cells by counting the number of intact nuclei in a hemacytometer (Farinelli et al., 1998; Stefanis et al., 1999). Cell counts were performed in triplicate.

2.8. *In vitro* assessment of calpain enzymatic activity

Six-day differentiated SH-SY5Y human neuroblastoma cells, grown in 6-well plates, were incubated with control CM or CM containing secreted AS for 8, 12, 16, and 24 hours. Recipient cells were washed with ice-cold PBS and homogenized in a buffer containing 10 mM HEPES (pH 7.5), 5 mM DTT, 1% NP-40 on ice for 30 minutes. Cell lysates (2 µg) were mixed with 25 µL of activity buffer (50 mM Tris-HCl [pH 7.6], 150 mM NaCl, 5 mM DTT, 10 mM CaCl₂) containing 10 µM fluorogenic calpain substrate (Calpain Substrate IV; Calbiochem, San Diego, CA, USA) and incubated at room temperature for 40 minutes in the dark. The reaction was stopped by adding 500 µL of 50 mM EDTA. Calpain activity was measured at 320 nm after excitation at 480 nm in a Perkin-Elmer LS-55 luminescence spectrometer (Perkin-Elmer, Norwalk, CT, USA). To test the specificity of the assay, 200 µM of the calpain inhibitor I A6185 (CI) was included where indicated (Banoczy et al., 2008).

2.9. 1-Pyrenedodecanoic acid fluorescence measurements

1-Pyrenedodecanoic acid labeling of plasma membranes and fluorescence measurements were carried out as described elsewhere (Galla and Luisetti, 1980; Hashimoto et al., 1999). SH-SY5Y cells were seeded on 6-well plates at a density of 1.0×10^5 cells per well, and differentiated for 6 days. Subsequently, cells were treated with secreted CM, WT– for 8 hours at 37 °C. At the end of the incubation period, cells were resuspended in PBS and transferred into a fluorimeter cuvette. 1-Pyrenedodecanoic acid (2 µM) was added for 5 minutes in the dark at room temperature (RT). After excitation at 340 nm, the fluorescence intensity was scanned from 380 to 580 nm in a luminescence spectrometer. The ratio of the maximum fluorescent intensity of excimer and pyrene monomers was calculated at 468 and 395 nm, respectively.

2.10. Free cytosolic Ca²⁺ measurements

Cells were loaded with Fura 2-AM as described (Papazafiri et al., 1994). Briefly, 6-day differentiated SH-SY5Y cells were treated with control or secreted CM, WT– for 8 hours, harvested in RPMI culture medium and centrifuged at 400g for 5 minutes at RT. Cell pellets were suspended in Krebs-Ringer-HEPES (KRH) buffer (125 mM NaCl, 5 mM KCl, 1.2 mM KH₂PO₄, 1.2 mM MgSO₄, 2 mM CaCl₂, 6 mM D-glucose, and 25 mM HEPES-NaOH [pH 7.4]) containing 2% FBS, counted in a hemocytometer and loaded with Fura 2-AM dye (2.5 µM), for 30 minutes at RT in the dark. Cells were resuspended in KRH supplemented with 250 mM sulfinpyrazone to prevent dye leakage, transferred to a thermostatted cuvette (37 °C), maintained in a continuous stirring condition, and analyzed in a Perkin-Elmer LS-55 luminescence spectrometer. To estimate capacitative calcium entry (CCE), 1.8×10^6 cells were resuspended in a CaCl₂-depleted KRH medium and 10 µM EGTA was added. Thapsigargin ([Tg] 100 nM) was added to deplete ER Ca²⁺ stores; CaCl₂ (3 mM) was reintroduced into the medium and the ensuing CCE was recorded. Results represent the maximal peak values normalized to ER content as exemplified by Tg-induced Ca²⁺ efflux of at least 3 independent experiments. Nifedipine ([nif] 1 µM), cntx (100 nM), or SKF (10 µM) was added after EGTA normalization and before the addition of Tg. VOCs were stimulated with 55 mM KCl, in the presence or absence of either 1 µM nif or 100 nM cntx. To estimate Ca²⁺ load in the diverse subcellular compartments, intracellular Ca²⁺ pools were depleted sequentially with the addition of the appropriate pharmacological compounds: 5 µM carbachole (Cch), followed by the addition of 100 nM Tg, 500 nM ionomycin (Iono), and 20 µM monensin A, in the presence or absence of extracellular Ca²⁺. To estimate the mitochondrial Ca²⁺ load, 1.8×10^6 Fura

2-loaded cells suspended in Ca²⁺-depleted KRH, were treated with 5 µM of the mitochondrial uncoupler FCCP, together with 2.5 µg/mL oligomycin (Oligo), to prevent ATP consumption via the reversed mode activity of the F1/F0 synthase.

2.11. Live Ca²⁺ imaging

For live Ca²⁺ imaging, 7-day-old rat cortical neurons (75,000 cells per chamber) plated on poly-L-lysine-coated 8-chamber slides (Integrated BioDiagnostics, Munich, Germany), were incubated with 2 µM Fura 2-AM in culture medium for 30 minutes at 37 °C, then returned to culture medium and incubated for 3 hours at 37 °C. Just before Ca²⁺ measurements, cells were washed once with microscopy buffer (129 mM NaCl, 5 mM KCl, 1 mM MgCl₂, 30 mM glucose, 1% BSA, 25 mM HEPES [pH 7.4]) and positioned in a temperature-controlled microscope. During measurements, CCE was assessed using stimulation with 0.25 µM Tg, followed by the addition of 6 mM CaCl₂. Fluorescence images obtained at 340 and 380 nm excitation and 510 nm emission were acquired by using a TE 2000U-inverted fluorescence microscope (Nikon, Osaka, Japan) coupled to a cooled charge-coupled device (CCD) camera (PTI-IC200) (Princeton Instruments). At the end of each experiment, the Fura 2-AM signals were calibrated with the simultaneous addition of 10 µM Iono and 50 mM KCl, to obtain the maximum fluorescence. Images were acquired every 10 seconds and cells were analyzed using the region of interest tool, to extract the fluorescence ratios. Changes in Ca²⁺ were determined using temporal analyses of single cells to express the data as fluorescence ratios as described (Smaili and Russell, 1999). The baseline fluorescence was determined at the beginning of each experiment by obtaining the average of the first 20 data points before compound addition, using the Image Master 3 Software (Graph-Pad Prism 4.0) acquisition-analysis software (PTI, Birmingham, NJ, USA). The results were normalized in relation to the baseline fluorescence and the data expressed as a percent of increase relative to baseline. The histograms represent the average peak response.

2.12. Statistical analysis

All data are expressed as mean ± standard error of the mean (SEM). Statistical analysis for multiple comparisons was performed using a 1-way analysis of variance followed by Tukey honestly significant difference (HSD) post hoc test. Nondirectional Student *t* tests were performed for comparisons involving only 2 groups. All statistical analyses were conducted using the Graph-Pad Prism software. Results were considered statistically significant at $p \leq 0.05$.

3. Results

3.1. Secreted AS induces an increase in capacitative Ca²⁺ entry in neuronally differentiated SH-SY5Y neuroblastoma cells

We wanted to investigate whether the mechanism via which secreted AS triggers the neurotoxic cascade involves alterations in the Ca²⁺ homeostatic machinery. As a source of cell-secreted AS, we used CM from SH-SY5Y cells inducibly overexpressing human WT AS (Emmanouilidou et al., 2010; Vekrellis et al., 2009). To elucidate the events that precede AS-induced cell death, we applied CM from the induced (CM, WT–) or the control uninduced cells (CM, WT+) to differentiated SH-SY5Y cells for 8 hours, because this was the longest incubation time during which the recipient cells did not exhibit any morphological or biochemical characteristics of cell degeneration (data not shown). After the 8-hour treatment, free cytosolic Ca²⁺ ([Ca²⁺]_i) recordings of the recipient cells were obtained using the Fura 2-AM dye. After ER depletion by Tg (100 nM), we measured CCE using exogenous

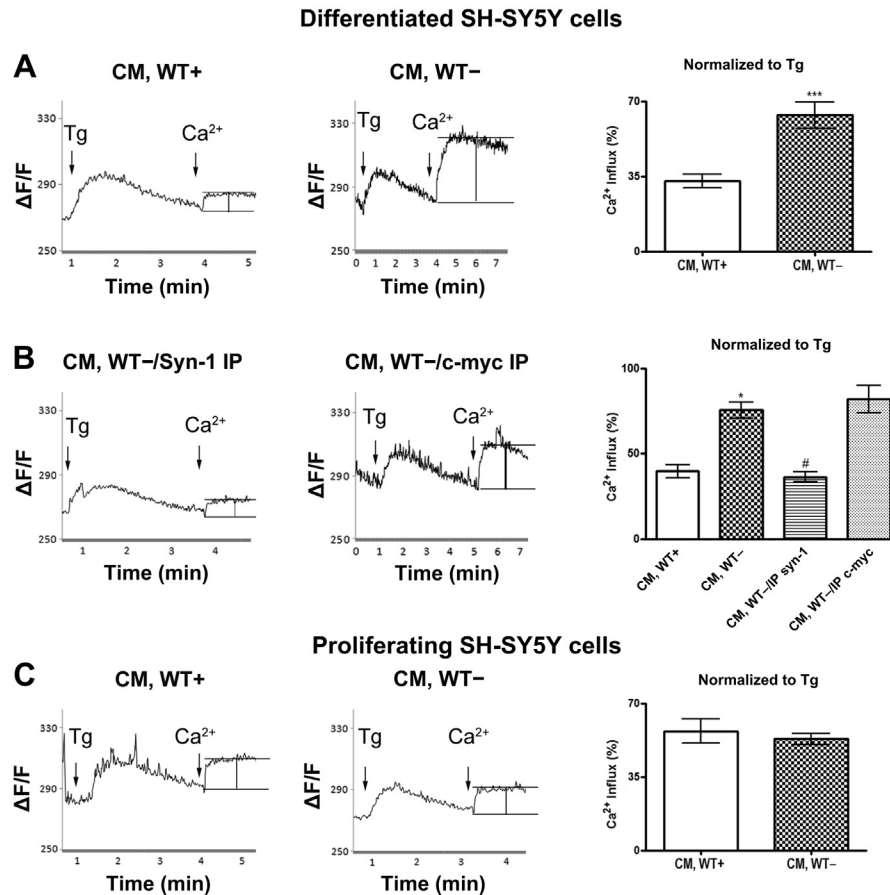


Fig. 1. Application of secreted AS increases CCE in differentiated, but not in proliferating recipient SH-SY5Y cells. (A) Differentiated SH-SY5Y cells were treated with CM, WT- or CM, WT+ for 8 hours and CCE was measured as described. Representative Ca^{2+} measurements depicting CCE are shown in the left panel and quantitative analysis of the percentage of Ca^{2+} influx, normalized to Tg-evoked Ca^{2+} release (first peak), is depicted in the right panel ($n = 16$; *** $p < 0.001$). (B) Differentiated SH-SY5Y cells were treated with AS-depleted (CM, WT-/Syn-1 IP) or control immunodepleted (CM, WT-/c-myc IP) CM for 8 hours. Representative Ca^{2+} measurements are shown in the left panel and quantitative analysis of the percentage of Ca^{2+} influx is depicted in the right panel ($n = 3$; * $p < 0.05$, comparing cells treated with CM, WT+ and CM, WT-; # $p < 0.05$, comparing between cells treated with CM, WT-/Syn-1 IP and cells treated with CM, WT-/c-myc IP). (C) Proliferating SH-SY5Y cells were treated with CM, WT- or CM, WT+ for 8 hours. The difference in percentage of Ca^{2+} influx between cells treated with CM, WT+ and CM, WT- was not statistically significant ($n = 3$). Abbreviations: AS, α -synuclein; Ca^{2+} , calcium; CCE, capacitative calcium entry; CM, conditioned medium; CM, WT+, control CM; CM, WT-, AS-containing medium; c-myc IP, control immunoprecipitation; F/F, fluorescence ratio; Syn-1 IP, alpha-synuclein immunoprecipitation; Tg, thapsigargin.

addition of 3 mM CaCl_2 (Fig. 1). Treatment of differentiated SH-SY5Y cells with the secreted CM, WT- resulted in a statistically significant increase in $[\text{Ca}^{2+}]_i$, compared with cultures incubated with CM, WT+ (Fig. 1A). Importantly, this increase in CCE was AS-dependent, because effective immunodepletion of AS from the CM, before its application to recipient cells, greatly reduced the Tg-evoked Ca^{2+} entry (Fig. 1B). Control immunodepletion with an irrelevant antibody (c-myc) failed to reduce CCE. In contrast, incubation of proliferating SH-SY5Y cells with the CM, WT+ or the CM, WT- resulted in similar CCE responses (Fig. 1C), suggesting that secreted AS only disturbs Ca^{2+} homeostasis in cells that have a neuronal phenotype.

3.2. Secreted AS-induced increase in Ca^{2+} entry is amplified by the L- and the N-type voltage-operated Ca^{2+} channels

In neurons, as in many other cell types, Ca^{2+} ions can enter cells via a number of channels, such as storage-operated channels (SOCs), VOCs, and receptor-operated plasma membrane Ca^{2+} channels. To assess the contribution of such channels to the AS-facilitated Ca^{2+} entry, we first examined the participation of SOC by blocking them with the SOC-specific inhibitor, SKF (10 μM). Addition of SKF resulted in a significant reduction in CCE, in

secreted AS- and control CM-treated cultures (Fig. 2A and B). However, the difference in CCE between the 2 groups in the presence of SKF, was maintained (Fig. 2B), implying that other plasma membrane channels might participate in the observed Ca^{2+} entry in the presence of secreted AS.

Previous reports have suggested that AS modulates the function of VOCs (Adamczyk and Strosznajder, 2006; Hettiarachchi et al., 2009; Kang et al., 2012). To test such a hypothesis in our cellular system, we used the L- and N-type specific VOC blockers, nif (1 μM) and cntx (100 nM), respectively. We found that nif and cntx reduced the Tg-evoked Ca^{2+} entry, only in cells treated with secreted AS (Fig. 2C and D). These results imply a participation of both L- and N-type Ca^{2+} channels in the observed CCE increase. Neither inhibitor affected the CCE of cells treated with the CM, WT+. Based on these findings we could surmise that in the presence of extracellular AS, VOCs might become active, thereby contributing to the SOC-facilitated Ca^{2+} entry.

To directly investigate the role of VOCs, we stimulated the cells with 55 mM KCl. Control and AS-treated cells responded to KCl stimulation robustly, yet Ca^{2+} entry was significantly greater in the latter (Fig. 2E and F). Addition of either nif or cntx, significantly reduced KCl-induced Ca^{2+} entry in both groups, verifying the functionality of these channels. Notably, the

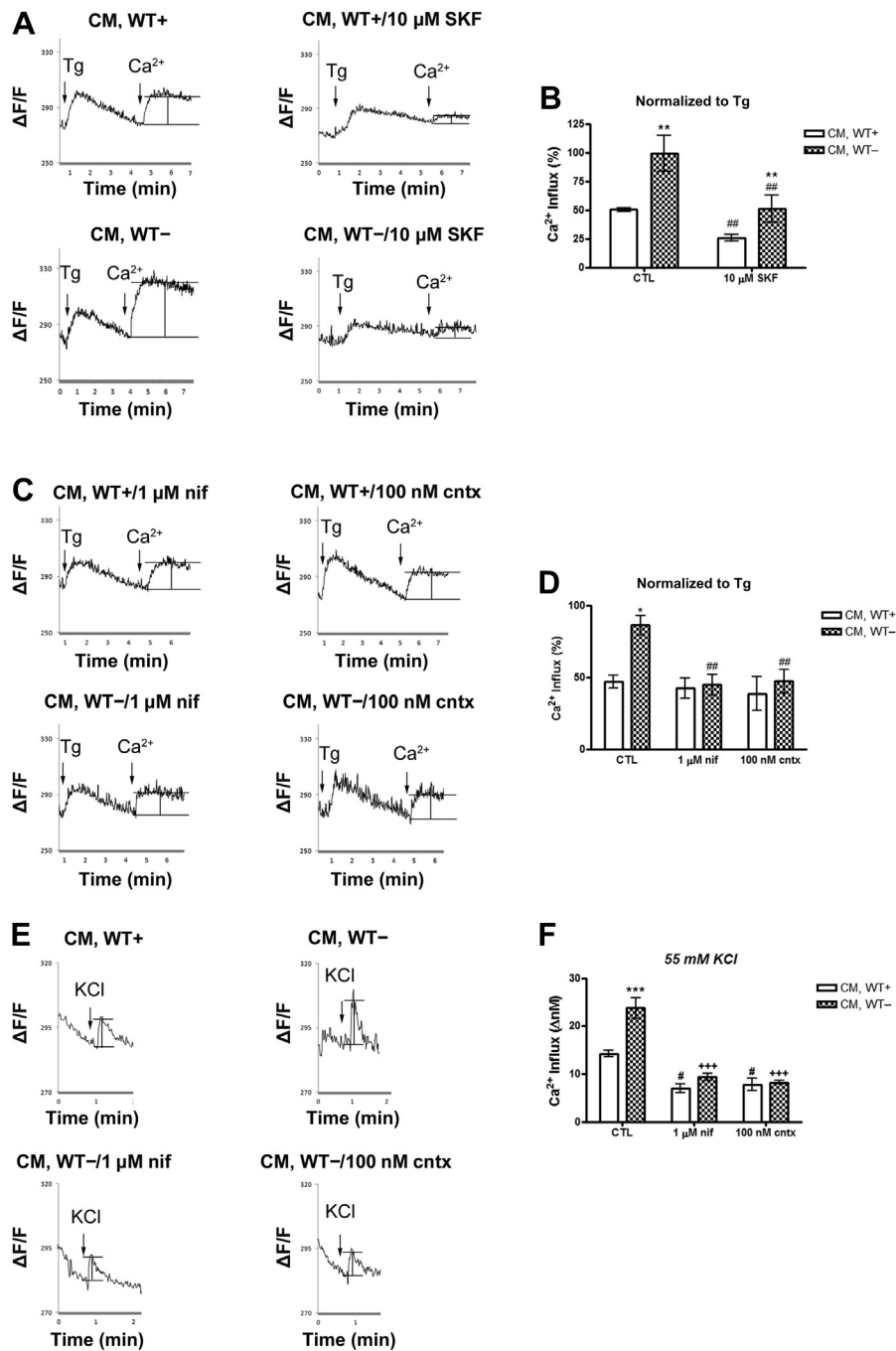


Fig. 2. L-type and N-type VOCs are implicated in the observed secreted AS-induced Ca²⁺ entry. Differentiated SH-SY5Y cells were treated with CM from AS-expressing (CM, WT-) or control (CM, WT+) cells for 8 hours. (A and C) Representative Ca²⁺ measurements depicting CCE in the absence or presence of SKF (A) and nif or cntx (C). (B and D) Quantitative analysis of the percentage of Ca²⁺ influx normalized to Tg-evoked Ca²⁺ release (first peak) between groups in the presence/absence of SKF (B) ($n = 4$, in duplicate; ** $p < 0.01$, comparing cells treated with CM, WT+ and CM, WT- in the presence/absence of SKF; ## $p < 0.01$ comparing SKF-treated and SKF-untreated cells) and nif or cntx (D) ($n = 5$, in duplicate; * $p < 0.05$, comparing cells treated with CM, WT+ and CM, WT-; ## $p < 0.01$ comparing cells treated with CM, WT- in the presence or absence of nif or cntx). (E) Representative Ca²⁺ recordings on KCl stimulation in the presence or absence of nif or cntx. (F) Quantification of Ca²⁺ influx (ΔnM) after KCl addition, in the presence or absence of the inhibitors ($n = 4$, in duplicate; *** $p < 0.001$, comparing cells treated with CM, WT+ and CM, WT-; # $p < 0.05$ comparing cells treated with CM, WT+ in the presence or absence of nif or cntx; +++ $p < 0.001$, comparing cells treated with CM, WT- in the presence or absence of the inhibitors). Abbreviations: AS, α -synuclein; Ca²⁺, calcium; CCE, capacitative calcium entry; CM, conditioned medium; CM, WT+, control CM; CM, WT-, AS-containing medium; cntx, ω -conotoxin GVIA; F/F, fluorescence ratio; nif, nifedipine; SKF, SKF 96365 hydrochloride; Tg, thapsigargin; VOC, voltage-operated Ca²⁺ channel.

difference in Ca²⁺ influx between control and AS-treated cells was abolished in the presence of VOC inhibitors (Fig. 2F), highlighting the important role of these channels in secreted AS-facilitated Ca²⁺ entry.

3.3. Naturally secreted AS induces mitochondrial Ca²⁺ uptake

Increased intracellular AS, and prefibrillar forms of recombinant AS, have been shown to induce high plasma membrane ion

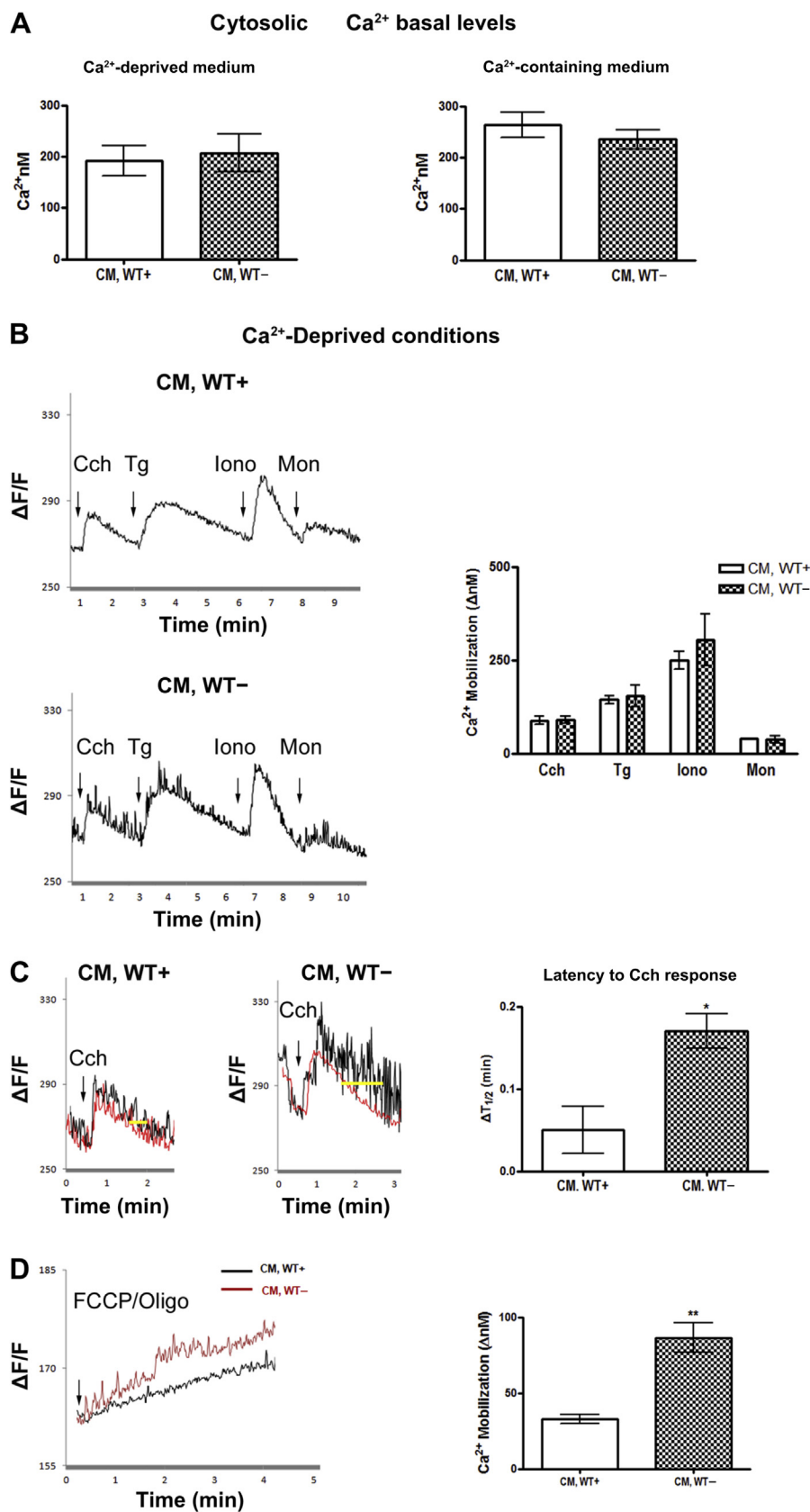


Fig. 3. AS-facilitated Ca^{2+} entry is driven to the mitochondria. Differentiated SH-SY5Y cells were treated with secreted CM, WT- or CM, WT+ for 8 hours, after labeling with Fura 2-AM. (A) The concentration of free cytosolic Ca^{2+} was estimated in Ca^{2+} -deprived conditions (left panel) and Ca^{2+} -containing conditions (right panel). No significant difference between the cells treated with CM, WT+ or with the CM, WT- was observed in either condition ($n = 3$, for Ca^{2+} -deprived conditions; $n = 11$, for Ca^{2+} -containing conditions). (B) Representative Ca^{2+} recordings depicting changes in $[\text{Ca}^{2+}]_i$ on sequential application of Cch, Tg, Iono, and Mon in Ca^{2+} -deprived conditions (left panel). Quantitative analysis of Ca^{2+} mobilization on addition of the compounds in the cells treated with CM, WT+ and CM, WT- in Ca^{2+} -deprived (right panel, $n = 3$), no statistical significant difference in Ca^{2+}

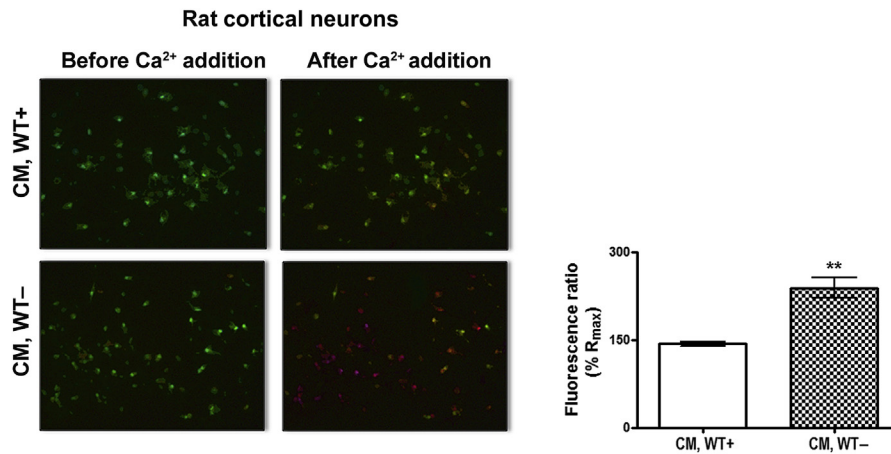


Fig. 4. Treatment with naturally secreted AS increases Ca^{2+} entry in primary rat cortical neurons. Seven-day-old rat cortical neurons were treated with secreted CM, WT⁻ or CM, WT⁺ for 8 hours. After loading with Fura 2-AM dye, CCE was monitored using a fluorescence microscope. Representative images illustrating the 350/380 fluorescence ratio before and after Ca^{2+} administration are shown in the left panel and quantitative analysis of the percentage of fluorescence ratio, normalized to baseline fluorescence, is depicted in the right panel ($n = 3$; ** $p < 0.005$). Abbreviations: AS, α -synuclein; Ca^{2+} , calcium; CCE, capacitative calcium entry; CM, conditioned medium; CM, WT⁺, control CM; CM, WT⁻, AS-containing medium; % R_{max} , percent of increase relative to baseline.

permeability and subsequent $[\text{Ca}^{2+}]_i$ rise (Danzer et al., 2007; Furukawa et al., 2006). Taking these, and our results, into account, we investigated whether the increased Ca^{2+} entry could lead to a subsequent rise in $[\text{Ca}^{2+}]_i$ levels. To this end, differentiated SH-SY5Y cells were treated as previously described and $[\text{Ca}^{2+}]_i$ levels were examined in Ca^{2+} -free and Ca^{2+} -containing environments. No significant difference in $[\text{Ca}^{2+}]_i$ was observed between AS-treated and control-treated cells in either condition (Fig. 3A).

Next, we asked whether the increased Ca^{2+} entry could lead to sequestration into specific intracellular Ca^{2+} pools. Under Ca^{2+} -depleted conditions, we first added Cch (5 μM), a cholinergic agonist that activates inositol trisphosphate receptor (IP_3R), resulting in Ca^{2+} efflux from the ER to the cytosol. When the Cch response was buffered, Tg (100 nM), a noncompetitive inhibitor of sarcoendoplasmic reticulum (SR) calcium transport ATPase (SERCA) pumps, was added to allow total ER Ca^{2+} depletion. Subsequently, we administered 500 nM Iono, a Ca^{2+} ionophore. After the Iono-evoked response, 20 μM of the sodium ionophore (Na^+/H^+ exchanger), monensin A, was added to release Ca^{2+} from acidic compartments, such as lysosomes. A representative Ca^{2+} trace after sequential addition of the examined agents is shown in Fig. 3B. Quantification of Ca^{2+} mobilization (i.e., Ca^{2+} rise), after the administration of each drug, revealed no statistically significant differences between AS-treated and control cells (Fig. 3C). Similar results were obtained in Ca^{2+} -containing conditions (data not shown).

Additionally, to further support our data regarding AS-induced Ca^{2+} entry, we investigated Cch-induced Ca^{2+} mobilization kinetics in differentiated cells exposed to secreted CM, WT⁻ and CM, WT⁺. Interestingly, the rate of Ca^{2+} buffering after stimulation with Cch in Ca^{2+} -containing compared with Ca^{2+} -depleted conditions was significantly slower in AS-treated compared with control cells (Fig. 3D). Because Cch triggers Ca^{2+} influx from the extracellular space as a secondary effect, the observed latency further supports that CM, WT⁻ potentiates Ca^{2+} entry from the plasma membrane, not only after stimuli such as Tg, but also on more physiological stimulations such as Cch.

Altogether, these results show a facilitated calcium entry in cells cultured with CM, WT⁻, with no apparent preferential Ca^{2+} distribution in a subcellular compartment. However, it is important to note that there was a higher Iono-evoked Ca^{2+} release in AS-treated compared with control cells, in Ca^{2+} -depleted conditions (Fig. 3B, right panel). Although it did not reach statistical significance, this trend implies the participation of a different subcellular Ca^{2+} pool. Therefore, we examined whether the mitochondria could be a potential pool for Ca^{2+} sequestration. To this end, 5 μM of the mitochondrial uncoupler, FCCP, together with 2.5 $\mu\text{g}/\text{mL}$ Oligo were added to control and AS-treated cells. Oligo prevents ATP consumption via the reversed mode activity of the F1/F0 synthase. In Ca^{2+} -depleted conditions, addition of FCCP with Oligo discharges mitochondrial Ca^{2+} stores, causing a rise of cytosolic $[\text{Ca}^{2+}]_i$, which reflects the mitochondrial Ca^{2+} load (Hettiarachchi et al., 2009). Secreted AS-treated cells exhibited a more profound response to the FCCP/Oligo treatment (Fig. 3E). Quantification of the Ca^{2+} mobilization on drug administration (expressed as ΔnM $[\text{Ca}^{2+}]_i$ at 4 minutes after drug addition) revealed significantly higher levels of mitochondrial Ca^{2+} content in AS-treated cells compared with control cells (32.83 ± 2.97 and 86.36 ± 9.75 , comparing cells treated with CM, WT⁺ and CM, WT⁻, respectively) (Fig. 3E). These results suggest that on exposure of recipient cells to CM, WT⁻, part of the excessive Ca^{2+} entry is driven to the mitochondrial Ca^{2+} pool.

3.4. Cell-secreted AS leads to a profound increase in CCE in primary rat cortical neurons

We have previously shown that primary cortical neurons are also susceptible to secreted AS neurotoxic effects (Emmanouilidou et al., 2010). We further examined whether application of cell-secreted AS on primary rat cortical neurons had similar effects on Ca^{2+} influx. To this end, 7-day-old rat cortical neurons were treated with CM, WT⁻ or CM, WT⁺ for 8 hours, after loading with Fura 2-AM and changes in CCE were recorded. As shown in Fig. 4, cortical neurons receiving secreted AS exhibited a profound increase in

mobilization was observed. (C) Representative Ca^{2+} recordings from cells treated with CM, WT⁺ and CM, WT⁻ illustrating the response to Cch in Ca^{2+} -depleted (red curve) and Ca^{2+} -containing conditions (black curve). Quantitative analysis of the time lapse ($\Delta T_{1/2}$) in the Cch curve revealed a significant delay in the decay of Cch-evoked Ca^{2+} release in the cells treated with CM, WT⁻ in Ca^{2+} -containing conditions, compared with the control-treated cells ($n = 3$; * $p < 0.05$). (D) Representative Ca^{2+} traces on addition of FCCP/Oligo in Ca^{2+} -depleted conditions (left panel). Graph depicting Ca^{2+} mobilization (ΔnM) after the discharge of mitochondrial Ca^{2+} stores (right panel). A significant increase of Ca^{2+} mobilization after FCCP/Oligo addition in the cells treated with CM, WT⁻ was observed ($n = 3$, in duplicate; ** $p < 0.01$). Abbreviations: AS, α -synuclein; Ca^{2+} , calcium; $[\text{Ca}^{2+}]_i$, free cytosolic Ca^{2+} ; Cch, carbachole; CM, conditioned medium; CM, WT⁺, control CM; CM, WT⁻, AS-containing medium; F/F, fluorescence ratio; FCCP, carbonyl cyanide p-trifluoromethoxy-phenylhydrazone; Iono, ionomycin; Mon, monensin A; Oligo, oligomycin; Tg, thapsigargin.

Ca²⁺ entry compared with control cells (percent of fluorescence ratio 143.3 ± 3.79 or 238.7 ± 17.5 in cells treated with CM, WT+ and CM, WT-, respectively), confirming the results obtained with differentiated SH-SY5Y cells.

3.5. Reduction of cytosolic Ca²⁺ levels protects from secreted AS-induced neurotoxicity

To investigate whether extracellular AS mediates its pathogenic actions through increased Ca²⁺ influx, we used chemical compounds that chelate intracellular or extracellular Ca²⁺ or prohibit Ca²⁺ from entering the cell. Six-day differentiated SH-SY5Y cells (Fig. 5A) and 7-day-old rat cortical neurons (Fig. 5D) were incubated for 24 hours at 37 °C with CM, WT- or CM, WT+, in the presence or absence of nif or cntx, and the intracellular or extracellular Ca²⁺ chelators, BAPTA-AM (BAPTA) or EGTA, respectively. In both cell types, the presence of extracellular AS led to a decrease in neuronal survival, which was mitigated on addition of either nif, cntx, BAPTA,

or EGTA (Fig. 5A and D). Drug application had no background toxicity, confirmed in control experiments.

To decipher whether AS-induced Ca²⁺ deregulation is directly linked to the observed cell death, Ca²⁺ modulators were added for the first 8 hours together with CM, WT-. Subsequently, the compounds were removed and CM, WT- was added to the cells for additional 8 or 16 hours. We found that the 8-hour treatment with the chelating compounds and the VOC inhibitors was sufficient to protect differentiated cells from AS-mediated toxicity at all time points (Fig. 5B and C). These results indicate that disturbances in Ca²⁺ homeostasis are the primary event in AS-triggered neurotoxic cascade.

3.6. Calpain activation is implicated in the extracellular AS-evoked neurotoxic effects

We have previously shown that treatment of neuronal cells with secreted AS results in caspase-3 cleavage (Emmanouilidou et al.,

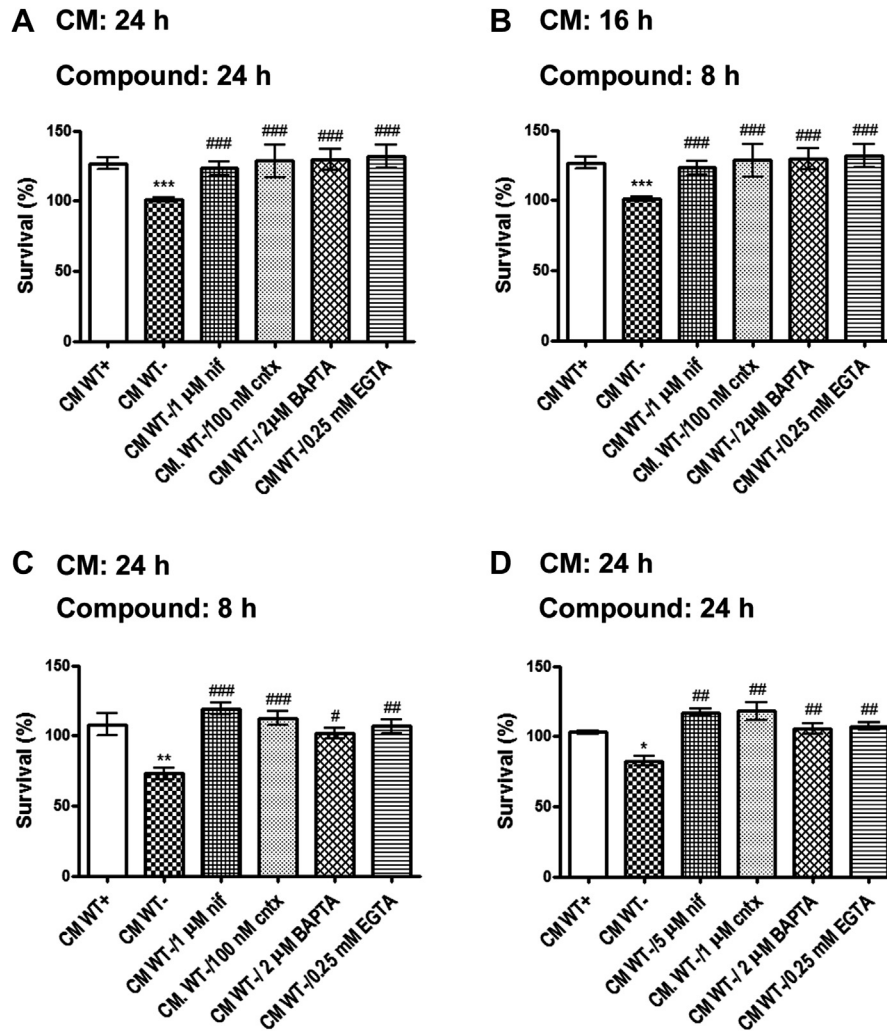


Fig. 5. Reduction of cytosolic Ca²⁺ levels protects neuronal cells against secreted AS-mediated neurotoxicity. (A–C) Differentiated SH-SY5Y cells were incubated with secreted CM, WT- or CM, WT+ for 24 hours (A, and C) or 16 hours (B), in the absence or presence of Ca²⁺ modulators. Neuronal survival was estimated by counting the number of intact nuclei in all conditions. All compounds significantly increased viability ($n = 3$, in triplicate; *** $p < 0.001$ for cells treated with CM, WT+ versus CM, WT-; ### $p < 0.001$ for cells treated with CM, WT- in the presence or absence of Ca²⁺ modulators, # $p < 0.05$ comparing AS-treated cells in the presence or absence of BAPTA). (D) Seven-day-old rat primary cortical neurons were treated with CM, WT- or CM, WT+, in the presence or absence of Ca²⁺ modulators for 24 hours and neuronal survival was measured using the same method. All compounds had a protective effect on cultures treated with CM, WT- ($n = 4$, in triplicate; * $p < 0.05$, for cells treated with CM, WT+ vs. CM, WT-, using unpaired t test; ## $p < 0.01$, for cells treated with CM, WT- in the absence/presence of Ca²⁺ modulators). All data are corrected to the baseline of control cells treated with CM, WT+. Abbreviations: AS, α -synuclein; Ca²⁺, calcium; CM, conditioned medium; CM, WT+, control CM; CM, WT-, AS-containing medium.

2010). Because calpains have been reported to cleave pro-caspase-3 (Camins et al., 2006) and to be activated in the setting of excess Ca^{2+} , we aimed to examine whether calpains are involved in the secreted AS-induced neurotoxicity. We incubated differentiated SH-SY5Y cells with CM, WT⁻, CM, WT⁺, or unconditioned medium (vehicle) for 8, 16, and 24 hours. Calpain activity was determined in the homogenates of the recipient cells using a calpain-specific fluorogenic substrate. As depicted in Fig. 6A, a statistically significant increase in calpain activity was observed after 24-hour incubation with AS (393.7 ± 45.03 , 499.8 ± 17.31 , and 679.7 ± 30.47 , for the cells treated with vehicle, CM, WT⁺, and CM, WT⁻, respectively). The specificity of the reaction was verified by the addition of the specific CI, which, as expected, resulted in a significant decrease of calpain activity (Fig. 6A, right panel).

We reasoned that if calpains are indeed activated during the process of AS-induced toxicity, their inactivation should result in an increase of cell survival after AS treatment. To test this hypothesis, we incubated cells with CM, WT⁻ in the presence or absence of the CI, for 24 hours. Addition of 1 μM CI greatly improved cell morphology (data not shown) and significantly increased cell viability (Fig. 6B). In a similar fashion to the survival assays with the Ca^{2+} modulators, we investigated whether calpain activation is a primary event for the observed death. CI was added for 8 hours together with the CM, WT⁻. Then, the inhibitor was removed and the cells were incubated for an additional 8 hours or 16 hours with CM, WT⁻ alone. Such treatment showed a trend of protection, after 16-hour incubation with CM, WT⁻ (82.38 ± 3.57 and 94.75 ± 4.39 ,

for the cells treated CM, WT⁻, in the absence or presence of CI, respectively) (Fig. 6C), but reached statistical significance only after 24 hours of incubation (74.25 ± 4.40 and 118.8 ± 3.58 , for the cells treated CM, WT⁻, in the absence or presence of CI, respectively) (Fig. 6D).

Similar experiments were performed in rat cortical cultures treated with CM, WT⁻ in the presence or absence of the CI for 24 hours. Such treatment showed that calpain inhibition also improved the survival of primary neurons exposed to AS, however, this effect did not reach statistical significance (Fig. 6E).

3.7. Interaction of secreted AS with the plasma membrane of recipient cells

In our previous work, we showed that secreted AS could exert its deleterious effects without frank internalization by differentiated SH-SY5Y cells (Emmanouilidou et al., 2010). Hence we wanted to investigate a potential association between AS and the plasma membrane of recipient cells. To do so, we examined changes in the microfluidic properties of the membrane of AS-treated cells. Cells were treated with CM from induced AS-overexpressing cells, or uninduced cells for 8 hours and incubated with 1-pyrenedodecanoic acid (2 μM). 1-Pyrenedodecanoic acid excimers break into monomers in the lipophilic interior of the membrane giving a distinct fluorescence spectrum that is indicative of the microfluidic properties of the membrane (Dafnis et al.,

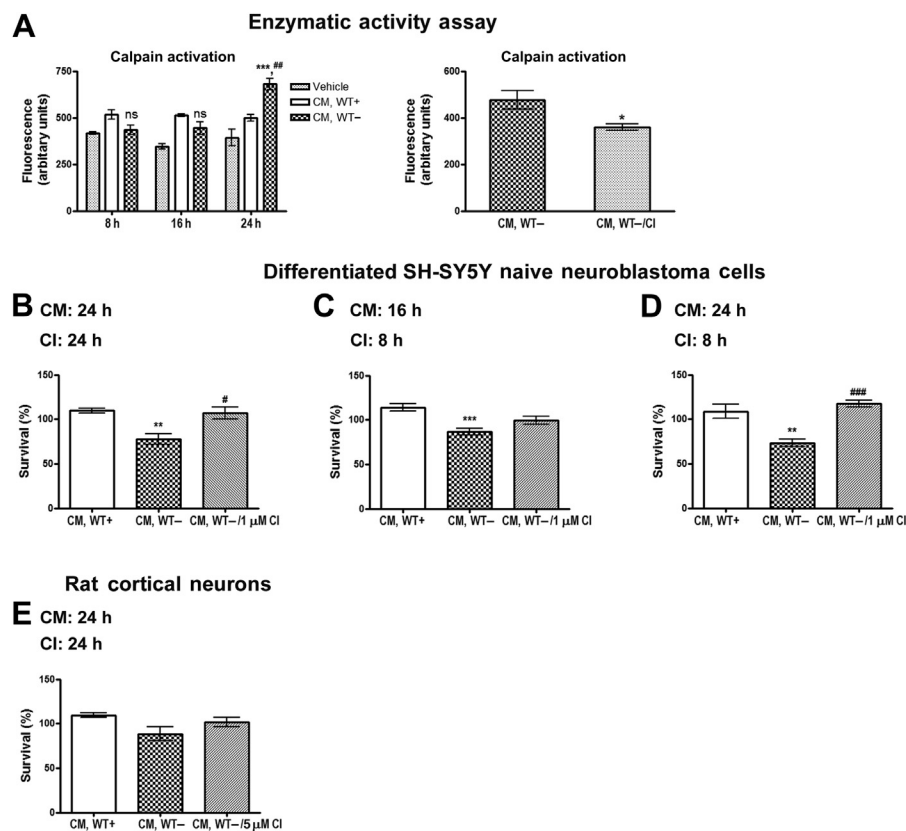


Fig. 6. Activation of calpains in recipient cells is a late effect of secreted AS. (A) Differentiated SH-SY5Y cells were incubated with CM, WT⁻, CM, WT⁺, or unconditioned medium (vehicle) for 8, 16, and 24 hours. (Left panel) Increased calpain activation was detected in AS-treated cells ($n = 3$; $*** p < 0.001$, comparing cells treated with vehicle and CM, WT⁻; $## p < 0.01$, comparing cells treated with CM, WT⁺ and CM, WT⁻). (Right panel) Specificity of the assay was verified using CI ($n = 4$; $* p < 0.05$, comparing cells treated with CM, WT⁻). (B–D) Quantitative analysis of the percentage of cell survival after treatment with CM, WT⁺ or CM, WT⁻ in the presence or absence of CI ($n = 4$ in triplicate for all time points). Statistics were performed using 1-way analysis of variance followed by Tukey's post hoc test ($** p < 0.01$ and $*** p < 0.001$, for cells treated with CM, WT⁺ vs. CM, WT⁻ in B, C, and D; $\# p < 0.05$ and $### p < 0.001$, for cells treated with CM, WT⁻ in the presence or absence of CI in B, and D). (E) Primary rat cortical neurons were incubated with CM, WT⁻ or CM, WT⁺ in the presence or absence of 5.0 μM CI for 24 hours. Abbreviations: AS, α -synuclein; CI, calpain inhibitor I A6185; CM, conditioned medium; CM, WT⁺, control CM; CM, WT⁻, AS-containing medium.

2010). The excimer to monomer ratio is an indicator of membrane fluidity with membrane rigidity bringing monomers in close proximity so as to create excised dimers, termed excimers. As shown in Fig. 7A, the excimer to monomer ratio is significantly reduced in AS-treated cells (1.488 ± 0.071 for CM, WT⁻, mean \pm SEM; $n = 6$) compared with CM, WT⁺-treated cells (1.725 ± 0.024 for CM, WT⁺, mean \pm SEM; $n = 6$), implying increased membrane fluidity. To exclude the possibility of dox interference in this setup, we collected CM from the Tet-Off parental SH-SY5Y line (2.22) expressing only the transactivator factor, in the absence or presence of dox. In both cases the excimer to monomer ratio was similar to that of the cells treated with the CM, WT⁺, suggesting that dox does not interfere with the fluidity assay. The ether phospholipid, miltefosine, known to directly interact and incorporate into the cell membrane, was used as a positive control for increased membrane fluidity (Fig. 7B).

3.8. The observed increase in Ca²⁺ entry is mostly attributed to the free extracellular- rather than the exosome-associated AS

Because AS is partly secreted via exosomes (Emmanouilidou et al., 2010), we finally sought to investigate the contribution of exosomes in the observed Ca²⁺ entry. We fractionated CM, WT⁻ and CM, WT⁺ into exosome-depleted supernatant (S100⁻ and S100⁺, respectively) and into exosome-enriched pellet (P100⁻ and P100⁺, respectively). Full CM and S100 supernatants were concentrated with using 3-kDa cutoff filters. P100 fractions were solubilized in RIPA buffer. Western blot analysis (Fig. 8A) revealed that only a small portion of secreted AS is present in the exosomal fraction, in accordance with our previous results (Emmanouilidou et al., 2010). Alix and flotillin-1 were used as biochemical markers for the exosome-enriched fraction, and BSA was used as loading control for CM and S100.

Exosomes from the CM, WT⁻ medium (P100⁻) were added in the S100⁺ supernatant from the CM, WT⁺ (S100⁺/P100⁻) and vice versa to yield an S100⁻/P100⁺ preparation. Cells were incubated with CM, WT⁻, control medium, or 1 of the previously described preparations (S100⁺, S100⁻, S100⁺/P100⁻, and S100⁻/P100⁺) for 8 hours. The recipient cells were loaded with Fura 2-AM, and ER depletion-induced Ca²⁺ influx was measured, as described earlier in text (Fig. 8B). Quantification of Ca²⁺ influx revealed that the observed increase is attributed largely to free extracellular AS (S100⁻) (percentage of Ca²⁺ influx, 117.2 ± 8.79 and 111.9 ± 10.87 , for cells treated with CM, WT⁻ and S100⁻, respectively). The addition of the exosome-associated AS (P100⁻) in the control S100⁺ supernatant did not significantly alter the CCE. This suggests that mainly free extracellular AS accounts for secreted AS-facilitated Ca²⁺ entry. This might be attributed to AS concentration, because only a small portion of secreted AS is packed in exosomes (Fig. 8A). Finally, the addition of P100⁺ to the S100⁻ did not lead to dramatic alterations of the CCE (percentage of Ca²⁺ influx 111.9 ± 10.87 and 101.3 ± 7.68 , for cells treated with S100⁻ and S100⁻/P100⁺, respectively), suggesting that the exosomes per se do not influence CCE.

4. Discussion

We have previously shown that cell-produced secreted AS is toxic to neuronal cells. Importantly, this toxicity did not appear to involve internalization of AS by the recipient neurons (Emmanouilidou et al., 2010). The aim of the current study was to investigate whether the effects of secreted AS on the recipient cells involve alterations at the level of the plasma membrane and deregulation of Ca²⁺ homeostasis.

To capture early events that could be pathologically relevant, the 8-hour treatment with CM containing secreted AS was chosen, because until that time point there are no overt signs of cellular degeneration. According to our results, 8-hour incubation with

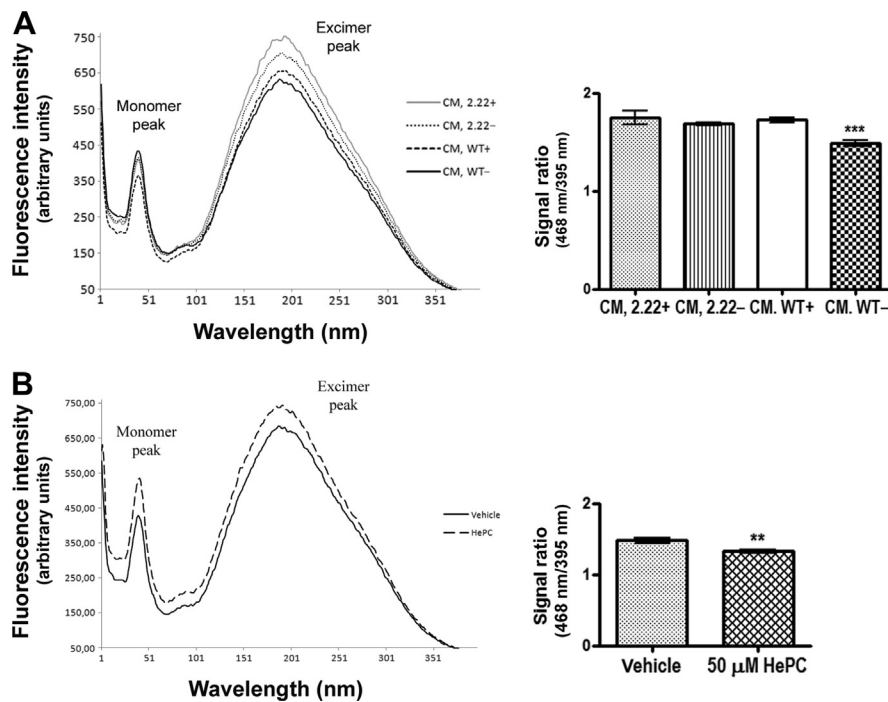


Fig. 7. Application of secreted AS-containing medium to neuronal cells affects their plasma membrane fluidity. (A) Differentiated SH-SY5Y cells were treated with CM, WT⁻ or control (CM, 2.22⁺, CM, 2.22⁻, CM, WT⁺) for 8 hours. Secreted AS induced changes in the microfluidic properties of the plasma membrane of the recipient cells. The graph depicts the excimer (468 nm) to monomer (395 nm) ratio ($n = 6$; *** $p < 0.001$ comparing the cells treated with CM, WT⁻ and control CMs [CM, 2.22⁺, CM, 2.22⁻, CM, WT⁺]). (B) Increased plasma membrane fluidity on treatment of differentiated SH-SY5Y cells with HePC for 8 hours ($n = 5$; ** $p < 0.01$, comparing the cells treated with vehicle and HePC, using unpaired t test). Abbreviations: AS, α -synuclein; CM, conditioned medium; CM, WT⁺, control CM; CM, WT⁻, AS-containing medium; HePC, miltefosine.

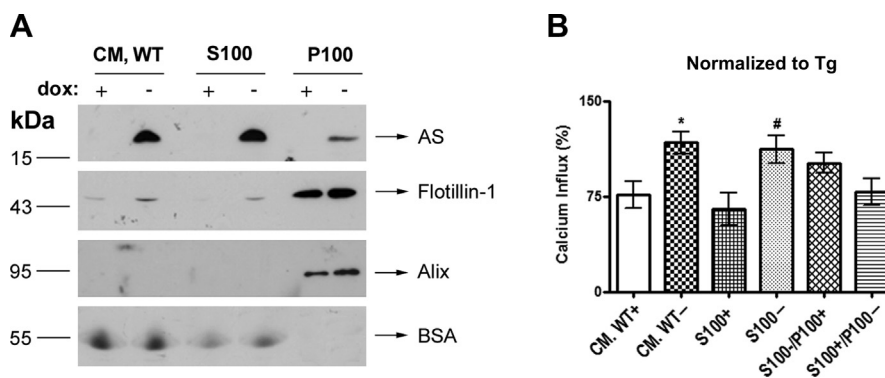


Fig. 8. Secreted AS-induced increase of CCE in recipient differentiated SH-SY5Y cells is mainly attributed to free AS. Control or secreted AS-containing CM was fractionated to yield exosome-depleted CM (S100+, S100-, respectively) and exosome-enriched pellet (P100). (A) CM, WT+/-, S100+/-, and P100+/- were analyzed using Western immunoblot with antibodies against AS, flotillin-1, alix, and BSA. (B) The P100 isolated from CM, WT- (P100-) was mixed with S100+ (S100+/P100-) and vice versa to create the S100-/P100+ preparation. Differentiated SH-SY5Y cells were treated either with CM, WT+ or CM, WT- or with one of the following preparations: S100+, S100-, S100+/P100-, S100-/P100+, for 8 hours and CCE was measured. The graph illustrates quantification of CCE normalized to Tg-evoked Ca^{2+} release ($n = 3$, in duplicate; * $p < 0.05$ comparing cells treated with CM, WT+ and cells treated with CM, WT-; # $p < 0.05$ comparing between cells treated with S100+ and cells receiving S100-, using unpaired t test). Abbreviations: AS, α -synuclein; BSA, bovine serum albumin; Ca^{2+} , calcium; CCE, capacitative calcium entry; CM, conditioned medium; CM, WT+, control CM; CM, WT-, AS-containing medium; dox, doxycycline; Tg, thapsigargin.

secreted AS was enough to cause Ca^{2+} perturbations, manifested by a significant increase in depleted ER-evoked Ca^{2+} entry (CCE), in differentiated SH-SY5Y cells and primary rat cortical neurons. The observed phenomenon greatly relies on the presence of secreted AS, because immunodepletion of the protein from the CM before administration to the cells does not alter CCE. Importantly, the presence of extracellular AS did not have any effect on the CCE of proliferating cells, which we have shown to be less susceptible to AS-conferred toxicity (Emmanouilidou et al., 2010). Additionally, reduction of cytosolic or extracellular Ca^{2+} levels via the BAPTA and EGTA Ca^{2+} chelators, respectively, spared recipient neuronal cells from AS-evoked toxicity. These data indicate that deregulation of Ca^{2+} homeostasis of the recipient cells is responsible, at least in part, for the neurotoxic potential of secreted AS. This raises the possibility that the differential toxic effects of secreted AS in neuronally differentiated versus proliferating cells (Emmanouilidou et al., 2010) might be related to its ability to alter Ca^{2+} homeostasis in the former, but not in the latter. Although an interplay between extracellular AS and alterations of Ca^{2+} homeostasis in the recipient cells has been suggested in previous reports, these were largely based on the use of recombinant AS; the current study is, to our knowledge, the first that etiologically links such early Ca^{2+} perturbations to secreted AS-mediated neurotoxicity.

To further elucidate the neurotoxic pathway triggered by secreted AS, we investigated the participation of plasma membrane Ca^{2+} channels. Because CCE was found to be increased in the presence of secreted AS, we sought to examine the involvement of SOCs. Although inhibition of SOCs by the specific inhibitor SKF, resulted in a significant reduction of CCE in control and AS-treated differentiated cells, the difference between the 2 groups in the presence of the inhibitor was not completely abolished. Such a finding implies that other plasma membrane channels could contribute to the AS-facilitated Ca^{2+} entry. Therefore we examined the role of the L- and N-type VOCs, using pharmacological inhibition with nif and cntx, respectively. Such treatment significantly reduces CCE to the control levels in differentiated cells, greatly alleviating AS-induced Ca^{2+} entry, suggestive of the involvement of VOCs in the observed phenomenon. In accordance with these findings, direct stimulation of VOCs by KCl depolarization led to a significantly higher Ca^{2+} influx in AS-treated cells compared with the control cells. Notably, inhibition of either L- or N-type VOCs greatly reduced Ca^{2+} influx on depolarization in both groups,

abolishing the difference between them. These findings prove the proper function of VOCs in the described cellular system and more importantly, verify the role of VOCs in secreted AS-evoked Ca^{2+} deregulation. Considering that we did not find any changes in the protein levels of VOCs (data not shown) on exposure of the cells to secreted AS, the described Ca^{2+} increase cannot be attributed to an upregulation of the expression levels of these channels. Instead, we saw that the presence of extracellular AS increased membrane fluidity of the recipient neuronal cells, potentially allowing the redistribution and clustering of plasma membrane receptors (including Ca^{2+} -dependent channels), which in turn might facilitate their activation and sensitivity to Ca^{2+} . Nonetheless, we cannot exclude the possibility of a direct interaction between secreted AS and the plasma membrane receptors, resulting in alteration of their function.

Because recombinant AS species have been shown to interact with artificial and biological membranes creating annular pores (Danzer et al., 2007; Tsigelny et al., 2012), we investigated the effect of AS on an Iono-evoked response. If the interaction of AS with the plasma membrane caused the formation of pores, the Iono-evoked response would result in a profound Ca^{2+} rise, in Ca^{2+} -containing conditions. Nevertheless, we found no significant difference in $[Ca^{2+}]_i$ between AS-treated and control cells suggesting that the likelihood of pore formation (at least at this early time point) is unlikely. However, we cannot exclude the possibility that such pores are formed at later time points (Schmidt et al., 2012; Tsigelny et al., 2012). The notion that secreted AS perturbs the normal function of the plasma membrane of the recipient cells, by facilitating increased Ca^{2+} influx, is further supported by the significantly slow buffering rate of the Cch-evoked Ca^{2+} rise in Ca^{2+} -containing compared with Ca^{2+} -depleted conditions, exhibited by AS-treated cells compared with the control cells.

Despite the profound increase in the observed Ca^{2+} entry, no significant changes in the steady-state levels of $[Ca^{2+}]_i$ were measured in AS-treated cells compared with control cells. Sequential Ca^{2+} release from the ER and the acidic stores did not reveal any striking differences in both Ca^{2+} -depleted and Ca^{2+} -containing conditions, excluding the possibility of alterations in Ca^{2+} mobilization. Direct discharge of the mitochondrial Ca^{2+} content using simultaneous administration of the mitochondrial uncoupler FCCP and Oligo, showed significantly increased Ca^{2+} sequestration in AS-treated cells, suggestive of mitochondrial Ca^{2+}

overload. It is possible that such overload might lead to mitochondrial dysfunction, thus linking extracellular AS and Ca^{2+} overload to the mitochondrial theory of PD pathogenesis (Benner et al., 2004; Cali et al., 2012; Vekrellis and Stefanis, 2012; Zhou et al., 2004).

Uncontrolled Ca^{2+} entry can result in the activation of calpains, a specific type of cysteine-protease that responds to Ca^{2+} signals (Medeiros et al., 2012). An increasing body of evidence gradually cements the notion that abnormal activation of calpains is 1 of the major culprits in a wide spectrum of brain disorders (Camins et al., 2006). However, the precise mechanism via which calpains regulate cell death pathways remains to be deciphered. Calpain activity was found to be increased in the protein preparations extracted from cells treated with AS for 24 hours, suggesting that calpain activation is a secondary event that follows Ca^{2+} deregulation. Considering that calpains can mediate caspase cleavage and activation (Camins et al., 2006), and that secreted AS-induced toxicity results in caspase-3 cleavage (Emmanouilidou et al., 2010), these data suggest a potential cross-talk between calpains and caspases. In our study, pharmacological inhibition of calpains protected neuronal cells from AS-induced death, further reinforcing the involvement of calpains in the described neurodegenerative process. However, this effect was more profound in differentiated SH-SY5Y cells than in rat cortical neurons, possibly because higher doses and more effective calpain inhibition were not achieved in the latter case, because of pharmacological toxicity observed with higher doses. In any case, the incomplete effects of calpain inhibition in rat cortical neurons suggest that other death pathways could contribute to the observed neurotoxicity.

It is important to note that an 8-hour treatment with chelating compounds (BAPTA, EGTA) and VOC inhibitors was enough to protect differentiated SH-SY5Y cells from 16 or 24 hours of total incubation with CM, WT-, thus placing Ca^{2+} deregulation at the beginning of the AS-triggered neurotoxic cascade. On the contrary, similar administration of CI started to be protective after the 16-hour incubation with CM, WT- and showed maximum protection after the 24-hour treatment. Taking into account the enzymatic activity data, which shows calpain activation after 16 hours of exposure to secreted AS, the above finding implies that calpains might be activated at 16 hours (albeit at low, nondetectable levels), but this activation was significant only at 24 hours. Therefore, it seems that calpain activation is 1 of the late events of the secreted AS-evoked neurotoxic cascade, downstream Ca^{2+} deregulation. However, further investigation is required to elucidate the precise involvement of calpains in this phenomenon.

We have shown that AS species can be delivered to the extracellular space, at least partly, via their association with exosomes. Measurements of CCE in recipient cells treated with free extracellular AS or exosome-associated AS preparations, revealed that free extracellular AS was more potent in inducing increased Ca^{2+} entry, compared with the exosome-associated protein. This difference in Ca^{2+} response might be because of the conformational changes that AS undergoes on packaging into exosomes which might affect its biochemical properties. In addition, considering that only a minor fraction of secreted AS is associated with exosomes (Danzer et al., 2012), this result might also reflect concentration differences.

Concluding, our findings indicate that secreted AS has neurotoxic effects, at least in part, through engagement of the Ca^{2+} homeostatic machinery. In this context, handling of Ca^{2+} signaling cascades might represent a potential therapeutic target for PD and related synucleinopathies by alleviating secreted AS-conferred neurotoxicity. Furthermore, our study provides a number of important novel mechanistic insights regarding the effect of secreted AS on neuronal cells. Initial effects leading to increased Ca^{2+} influx are linked to altered membrane fluidity, likely causing

clustering or oversensitization of VOCs, whereas pore formation does not appear to play a role at these early time points. In the further cascade of events, calpain activation and, possibly, mitochondrial Ca^{2+} overload, are important factors leading to neurotoxicity.

Disclosure statement

There is no actual or potential conflicts of interest related to the work presented in this manuscript.

All animals were handled according to the ethical standards of BRFAA under protocols approved by the Animal Care and Use Committee of the Institution and in accordance with the European Convention 123/Council of Europe and Directive 86/609/EEC.

Acknowledgements

The authors thank the BRFFA biological imaging facility for assistance with Ca^{2+} imaging experiments, and Dr Chroni for her technical advice on the setup of the membrane fluidity assay. This research was cofinanced by the European Union (European Social Fund – ESF) and Greek national funds of the National Strategic Reference Framework (NSRF) – Research Funding Program: Heracleitus II. Additional funding for this project was provided by MEFOPA, FP7.

References

- Adamczyk, A., Strosznajder, J.B., 2006. Alpha-synuclein potentiates Ca^{2+} influx through voltage-dependent Ca^{2+} channels. *Neuroreport* 17, 1883–1886.
- Banoczi, Z., Alexa, A., Farkas, A., Friedrich, P., Hudecz, F., 2008. Novel cell-penetrating calpain substrate. *Bioconjug. Chem.* 19, 1375–1381.
- Benner, E.J., Mosley, R.L., Destache, C.J., Lewis, T.B., Jackson-Lewis, V., Gorantla, S., Nemachek, C., Green, S.R., Przedborski, S., Gendelman, H.E., 2004. Therapeutic immunization protects dopaminergic neurons in a mouse model of Parkinson's disease. *Proc. Natl. Acad. Sci. U.S.A.* 101, 9435–9440.
- Berridge, M.J., Bootman, M.D., Roderick, H.L., 2003. Calcium signalling: dynamics, homeostasis and remodelling. *Nat. Rev. Mol. Cell Biol.* 4, 517–529.
- Cali, T., Ottolini, D., Negro, A., Brini, M., 2012. α -Synuclein controls mitochondrial calcium homeostasis by enhancing endoplasmic reticulum-mitochondria interactions. *J. Biol. Chem.* 287, 17914–17929.
- Camins, A., Verdaguier, E., Folch, J., Pallas, M., 2006. Involvement of calpain activation in neurodegenerative processes. *CNS Drug Rev.* 12, 135–148.
- Chivet, M., Hemming, F., Pernet-Gallay, K., Fraboulet, S., Sadoul, R., 2012. Emerging role of neuronal exosomes in the central nervous system. *Front. Physiol.* 3, 145.
- Churchill, G.C., Okada, Y., Thomas, J.M., Genazzani, A.A., Patel, S., Galione, A., 2002. NAADP mobilizes Ca^{2+} from reserve granules, lysosome-related organelles, in sea urchin eggs. *Cell* 111, 703–708.
- Dafnis, I., Stratikos, E., Tzinia, A., Tsilibary, E.C., Zannis, V.I., Chroni, A., 2010. An apolipoprotein E4 fragment can promote intracellular accumulation of amyloid peptide beta 42. *J. Neurochem.* 115, 873–884.
- Danzer, K.M., Haasen, D., Karow, A.R., Moussaud, S., Habeck, M., Giese, A., Kretschmar, H., Hengerer, B., Kostka, M., 2007. Different species of alpha-synuclein oligomers induce calcium influx and seeding. *J. Neurosci.* 27, 9220–9232.
- Danzer, K.M., Kranich, L.R., Ruf, W.P., Cagsal-Getkin, O., Winslow, A.R., Zhu, L., Vanderburg, C.R., McLean, P.J., 2012. Exosomal cell-to-cell transmission of alpha-synuclein oligomers. *Mol. Neurodegener.* 7, 42.
- Dauer, W., Przedborski, S., 2003. Parkinson's disease: mechanisms and models. *Neuron* 39, 889–909.
- de Brito, O.M., Scorrano, L., 2008. Mitofusin 2 tethers endoplasmic reticulum to mitochondria. *Nature* 456, 605–610.
- Demuro, A., Parker, I., Stutzmann, G.E., 2010. Calcium signaling and amyloid toxicity in Alzheimer disease. *J. Biol. Chem.* 285, 12463–12468.
- Emmanouilidou, E., Melachroinou, K., Roumeliotis, T., Garbis, S.D., Ntzouni, M., Margaritis, L.H., Stefanis, L., Vekrellis, K., 2010. Cell-produced alpha-synuclein is secreted in a calcium-dependent manner by exosomes and impacts neuronal survival. *J. Neurosci.* 30, 6838–6851.
- Farinelli, S.E., Greene, L.A., Friedman, W.J., 1998. Neuroprotective actions of dipyrindamole on cultured CNS neurons. *J. Neurosci.* 18, 5112–5123.
- Furukawa, K., Matsuzaki-Kobayashi, M., Hasegawa, T., Kikuchi, A., Sugeno, N., Itoyama, Y., Wang, Y., Yao, P.J., Bushlin, I., Takeda, A., 2006. Plasma membrane ion permeability induced by mutant alpha-synuclein contributes to the degeneration of neural cells. *J. Neurochem.* 97, 1071–1077.

- Galla, H.J., Luisetti, J., 1980. Lateral and transversal diffusion and phase transitions in erythrocyte membranes. An excimer fluorescence study. *Biochim. Biophys. Acta* 596, 108–117.
- Gasser, T., 2009. Molecular pathogenesis of Parkinson disease: insights from genetic studies. *Expert Rev. Mol. Med.* 11, e22.
- Greer, P.L., Greenberg, M.E., 2008. From synapse to nucleus: calcium-dependent gene transcription in the control of synapse development and function. *Neuron* 59, 846–860.
- Hashimoto, M., Hossain, S., Masumura, S., 1999. Effect of aging on plasma membrane fluidity of rat aortic endothelial cells. *Exp. Gerontol.* 34, 687–698.
- Hettiarachchi, N.T., Parker, A., Dallas, M.L., Pennington, K., Hung, C.C., Pearson, H.A., Boyle, J.P., Robinson, P., Peers, C., 2009. α -Synuclein modulation of Ca²⁺ signaling in human neuroblastoma (SH-SY5Y) cells. *J. Neurochem.* 111, 1192–1201.
- Kang, S., Cooper, G., Dunne, S.F., Dusel, B., Luan, C.H., Surmeier, D.J., Silverman, R.B., 2012. CaV1.3-selective L-type calcium channel antagonists as potential new therapeutics for Parkinson's disease. *Nat. Commun.* 3, 1146.
- Kordower, J.H., Chu, Y., Hauser, R.A., Olanow, C.W., Freeman, T.B., 2008. Transplanted dopaminergic neurons develop PD pathologic changes: a second case report. *Mov. Disord.* 23, 2303–2306.
- Lamarca, V., Scorrano, L., 2009. When separation means death: killing through the mitochondria, but starting from the endoplasmic reticulum. *EMBO J.* 28, 1681–1683.
- Li, J.Y., Englund, E., Holton, J.L., Soulet, D., Hagell, P., Lees, A.J., Lashley, T., Quinn, N.P., Rehnrota, S., Bjorklund, A., Widner, H., Revesz, T., Lindvall, O., Brundin, P., 2008. Lewy bodies in grafted neurons in subjects with Parkinson's disease suggest host-to-graft disease propagation. *Nat. Med.* 14, 501–503.
- Martin, Z.S., Neugebauer, V., Dineley, K.T., Kaye, R., Zhang, W., Reese, L.C., Tagliatela, G., 2012. α -Synuclein oligomers oppose long-term potentiation and impair memory through a calcineurin-dependent mechanism: relevance to human synucleinopathies. *J. Neurochem.* 120, 440–452.
- Medeiros, R., Kitazawa, M., Chabrier, M.A., Cheng, D., Baglietto-Vargas, D., Kling, A., Moeller, A., Green, K.N., LaFerla, F.M., 2012. Calpain inhibitor A-705253 mitigates Alzheimer's disease-like pathology and cognitive decline in aged 3xTgAD mice. *Am. J. Pathol.* 181, 616–625.
- Nalls, M.A., Plagnol, V., Hernandez, D.G., Sharma, M., Sheerin, U.M., Saad, M., Simon-Sanchez, J., Schulte, C., Lesage, S., Sveinbjornsdottir, S., Stefansson, K., Martinez, M., Hardy, J., Heutink, P., Brice, A., Gasser, T., Singleton, A.B., Wood, N.W., 2011. Imputation of sequence variants for identification of genetic risks for Parkinson's disease: a meta-analysis of genome-wide association studies. *Lancet* 377, 641–649.
- Papazafiri, P., Bossi, M., Meldolesi, J., 1994. Expression of muscle calsequestrin in epithelial HeLa cells: distribution and functional role. *Biochim. Biophys. Acta* 1223, 333–340.
- Patel, S., Docampo, R., 2010. Acidic calcium stores open for business: expanding the potential for intracellular Ca²⁺ signaling. *Trends Cell Biol.* 20, 277–286.
- Schmidt, F., Levin, J., Kamp, F., Kretzschmar, H., Giese, A., Botzel, K., 2012. Single-channel electrophysiology reveals a distinct and uniform pore complex formed by alpha-synuclein oligomers in lipid membranes. *PLoS One* 7, e42545.
- Smaili, S.S., Russell, J.T., 1999. Permeability transition pore regulates both mitochondrial membrane potential and agonist-evoked Ca²⁺ signals in oligodendrocyte progenitors. *Cell Calcium* 26, 121–130.
- Spillantini, M.G., Schmidt, M.L., Lee, V.M., Trojanowski, J.Q., Jakes, R., Goedert, M., 1997. Alpha-synuclein in Lewy bodies. *Nature* 388, 839–840.
- Stefanis, L., Park, D.S., Friedman, W.J., Greene, L.A., 1999. Caspase-dependent and -independent death of camptothecin-treated embryonic cortical neurons. *J. Neurosci.* 19, 6235–6247.
- Surmeier, D.J., Guzman, J.N., Sanchez-Padilla, J., 2010. Calcium, cellular aging, and selective neuronal vulnerability in Parkinson's disease. *Cell Calcium* 47, 175–182.
- Thery, C., Amigorena, S., Raposo, G., Clayton, A., 2006. Isolation and characterization of exosomes from cell culture supernatants and biological fluids. *Curr. Protoc. Cell Biol.* Chapter 3, Unit 3.22.
- Tsigelny, I.F., Sharikov, Y., Wrasidlo, W., Gonzalez, T., Desplats, P.A., Crews, L., Spencer, B., Masliah, E., 2012. Role of alpha-synuclein penetration into the membrane in the mechanisms of oligomer pore formation. *FEBS J.* 279, 1000–1013.
- Vekrellis, K., Stefanis, L., 2012. Targeting intracellular and extracellular alpha-synuclein as a therapeutic strategy in Parkinson's disease and other synucleinopathies. *Expert Opin. Ther. Targets* 16, 421–432.
- Vekrellis, K., Xilouri, M., Emmanouilidou, E., Rideout, H.J., Stefanis, L., 2011. Pathological roles of alpha-synuclein in neurological disorders. *Lancet Neurol.* 10, 1015–1025.
- Vekrellis, K., Xilouri, M., Emmanouilidou, E., Stefanis, L., 2009. Inducible over-expression of wild type alpha-synuclein in human neuronal cells leads to caspase-dependent non-apoptotic death. *J. Neurochem.* 109, 1348–1362.
- Vogiatzi, T., Xilouri, M., Vekrellis, K., Stefanis, L., 2008. Wild type alpha-synuclein is degraded by chaperone-mediated autophagy and macroautophagy in neuronal cells. *J. Biol. Chem.* 283, 23542–23556.
- Yamasaki, M., Masgrau, R., Morgan, A.J., Churchill, G.C., Patel, S., Ashcroft, S.J., Galione, A., 2004. Organelle selection determines agonist-specific Ca²⁺ signals in pancreatic acinar and beta cells. *J. Biol. Chem.* 279, 7234–7240.
- Zhou, C., Emadi, S., Sierks, M.R., Messer, A., 2004. A human single-chain Fv intrabody blocks aberrant cellular effects of overexpressed alpha-synuclein. *Mol. Ther.* 10, 1023–1031.
- Zundorf, G., Reiser, G., 2011. Calcium dysregulation and homeostasis of neural calcium in the molecular mechanisms of neurodegenerative diseases provide multiple targets for neuroprotection. *Antiox. Redox Signal* 14, 1275–1288.